Supplementary Information (SI) for Catalysis Science & Technology.

Supporting Information

In Situ Preparation and Performance of Iron Based Electro-magnetic Synergistic Electrochemical Nitrogen Fixation Catalysts

Kaidi Chen, Run Deng, Chen Zhao, and Qikun Zhang*

Abstract: An iron based catalyst was prepared in situ in $FeSO_4$ solution by electrochemical technology to catalyze the reduction of N_2 to NH_3. $FeSO_4$ solution was not only used as the electrode position solution for preparing iron based catalyst, but also as the electrolyte for catalyzing the synthesis of ammonia from Electrochemical Nitrogen Reduction Reaction (ENRR). It was proved that the main component of the iron based catalyst was Fe (0), and the morphology of the prepared catalyst was lamellar structure. The ENRR performance was tested at different reaction potentials and different electrolyte concentrations, and the optimal reaction conditions were investigated. It was found for the first time that the applied magnetic field can significantly increase the current density. Thus, the yield and efficiency of electrochemical ammonia synthesis are significantly affected. When the potential was -1.0 V vs SCE, and the electrolyte was 0.3 mol /L $FeSO_4$ solution, the highest ammonia yield was 923±46 $mg\cdot h^{-1}\cdot m^{-2}$, and the highest faraday efficiency was 18.35%. This work simplifies the tedious and costly catalyst synthesis process and provides a new strategy for the industrial application of ENRR.

Experimental Procedures

In situ preparation of iron based catalysts

In this work, electrochemical technology is used to prepare iron based catalyst in situ and catalyze N_2 reduction to synthesize ammonia. The reaction device is shown in Figure S1. Ammonia is easily soluble in water and there are generally trace ammonia nitrogen pollutants in the atmosphere and environment. During the experiment of electrochemical ammonia synthesis, strict measures should be taken to eliminate the possible ammonia pollution. Fresh deionized water is used to prepare the solution needed for the experiment. Feed gas N_2 (high-purity, 99.999%) needs to pass through the gas washing bottle with 10 mL absorption liquid before being introduced into the electrolytic cell to ensure that the feed gas does not contain ammonia pollutants. The rear absorption bottle with 100 mL absorption liquid is connected behind the electrolytic cell to absorb the NH_3 that may be carried out with the air flow.

Effect of the applied magnetic field

An electromagnet is used to control the addition and removal of the external magnetic field**.** According to Ampère's Circuital Law, the flow of electric current produces a magnetic field around the conductor. The magnetic field lines circulate around the conductor in concentric loops. In this way, magnetic fields are generated and turned off as the power is switched on and off. The effect of an external magnetic field on the ammonia synthesis performance of the iron-based catalyst in this work was investigated.

Ammonia Detection

The yield of ammonia synthesis by electrochemical catalytic reduction of N_2 was determined by indophenol blue spectrophotometry (IBSP). The detection principle is that ammonia is absorbed in dilute sulfuric acid in the presence of sodium nitroferricyanide and sodium hypochlorite, and salicylic acid produces the indophenol blue dye, which is quantified according to a modified colorimetric method [1, 2]. In this experiment, a distillation device is used to extract and absorb NH_3 in electrolyte into dilute sulfuric acid by evaporation of water vapor, and then detect it by IBSP. The device is shown in Figure S2 which include a round bottom flask, a nitrogen ball, a straight condensing tube, and a conical flask. The specific protocols are as follows:

Preparation of standard solutions

Salicylic acid solution (5.0 Wt % aqueous solution): 10.0 g salicylic acid [C_6H_4 (OH) COOH] and 10.0 g sodium citrate [$Na_3C_6O_7 \cdot 2H_2O$] were weighed and added to a beaker with 50 mL deionized water, mixed with 55 mL 2 Mol·L^{-1} sodium hydroxide solution and diluted to 200 mL with deionized water.

Sodium nitroferricyanide solution (1.0 Wt% aqueous solution): 1.0 g sodium nitroferricyanide [$Na_2Fe(CN)_5 \cdot NO \cdot 2H_2O$] was added to a beaker with an appropriate volume of water, and after dissolving completely, was transfer to a volumetric flask with a final volume of 100 mL. The solution was stored in a refrigerator at 4°C and reconstituted after 30 days.

Sodium hypochlorite solution [0.05 mol·L^{-1}]: A 1.0 mL sodium hypochlorite solution was calibrated by iodometry. Then, it was diluted to 0.05 mol·L^{-1} with a 2 mol·L^{-1} sodium hydroxide solution. The solution was stored in a refrigerator at 4°C and reconstituted after 60 days.

Absorption solution [0.005 mol·L^{-1} H_2SO_4 aqueous solution]: 2.8 mL of concentrated sulfuric acid was taken and diluted to 1 L for a concentration of 0.05 mol·L^{-1}. When used, the final concentration was further diluted to 0.005 mol·L^{-1}.

Ammonia standard solution

Ammonium chloride (NH_4Cl), 0.3142 g, was dried at 105 °C for 1 h, dissolved in an appropriate volume of water, transferred into a 100 mL volumetric flask, and diluted with the 0.05 mol·L^{-1} absorption solution. The final concentration of ammonia in solution was 1.00 mg·mL^{-1}. When used, the above solution was diluted with the 0.005 mol·L^{-1} absorption solution to obtain a final concentration of ammonia of 1.00 μg·mL^{-1}.

Creation of a standard curve

Concentrations in colorimetric tubes for each color reaction are shown in Supplementary Table S1 and Figure S3. Various solutions were placed in seven 10 mL plugged colorimetric tubes. A 0.50 mL salicylic acid solution, 0.10 mL sodium nitroferrocyanide solution and 0.10 mL sodium hypochlorite solution were added to each colorimetric tube. After mixing evenly, the solution was reacted at 25 °C for 1.0 h. Water was the blank, and the absorbance of each tube solution was measured by a spectrophotometer at 697.5 nm in a 1.0 cm cuvette. Taking the ammonia concentration (mg·L^{-1}) as the abscissa and the absorbance as the ordinate, a standard curve was drawn. The linear equation of the regression line and the correlation coefficient of the standard curve were calculated. The standard curve equation was Y=0.87979X+0.03662, the linear correlation coefficient was R^2=0.9996, and the minimum detection concentration was 0.05 μg·mL^{-1} (Figure S4).

Detection of ammonia in samples

According to the same procedure of drawing the standard curve, 1.0 mL of sample was added to a plugged colorimetric tube and reacted with chromogenic substrates. The absorbance of the sample was determined accordingly. The concentration of ammonia in the sample was calculated according to the linear equation of the standard working curve, and the yield of electrocatalytic ammonia synthesis was calculated eventually.

Calculation of the yield rate and the faradaic efficiency of NH_3

The yield rate (Y.R., mg_{NH3} h^{-1} cm^{-2}) of NH_3 can be calculated using the following equation:

$$Y.R.(NH_3) = \frac{C_{NH3} \times V}{t \times A} \times 10^{-3} \quad (1)$$

The faradaic efficiency (F.E.) of NH_3 was the percentage of the charge consumed for NH_3 generation in the total charge passed through the electrode according to the equation below:

$$F.E.(NH_3) = \frac{3 \times F \times C_{NH3} \times V \times 10^{-6}}{17 \times Q} \times 100\% \quad (2)$$

where C_{NH3} is the measured NH_3 concentration (μg mL^{-1}); V is the volume of the electrolyte (30 mL); t is the electrolysis time (0.5 h); A is the geometric area of the electrode (1.4 cm^2); F is the faraday constant (96500 C mol^{-1}); Q (C) is the total charge passed through the electrode, which is the integral of I-t curve. The yield rate, the faradaic efficiency, and corresponding error bars were obtained from three individual samples under the same testing conditions.

Turnover frequency of ammonia

The turnover frequency (TOF, s^{-1}) of ammonia in ENRR process indicates the number of ammonia molecules produced per unit time and per active sites. Thus, TOF values can be calculated based on the yield rate (Y.R., mg_{NH3}·h^{-1}·cm^{-2}) and EASA-based site density ($D_{site\ density}$, atom μm_{EASA}^{-2}) as follows.

$$TOF = \frac{Y.R.(NH_3) \times N_A}{D_{site\ density} \times A_{EASA,CF} \times 17 \times 3600} \quad (3)$$

The calculation of EASA-based site density

The EASA-based site density ($D_{site\ density}$, atom μm_{EASA}^{-2}) was calculated according to the active site numbers and $A_{EASA,\ CF}$ of catalysts loaded on the CF shown below.

$$D_{site\ density} = \frac{(C_x - C_{1.2}) \times 10^6}{n \times A_{EASA,\ CF} \times F} \times N_A \quad (4)$$

where C_x and $C_{1.2}$ are the integrated charge (C) from potentiostatic curves at a specific substrate potential (x) and 1.2 V (as the background); n is the number of electrons for oxidizing Fe species (3 for Fe (0), 1 for Fe (II)); A_{EASA} is electrochemical active surface area of catalysts on the Cupper Foam (CF) determined in ENRR; F is faradic constant (96500 C mol^{-1}); N_A is the Avogadro constant (6.02×10^{23}).

The calculation of electrochemical active surface area

The electrochemical active surface area (A_{EASA}) of catalysts loaded on the Cupper Foam ($A_{EASA,\ CF}$, $cm^2 \cdot cm^{-2}$) was based on the ideal specific capacitance of metal electrode ($C_{EDLC,\ metal}$ = 30 μF cm^{-2}) according to the following equation:

$$A_{EASA} = \frac{C_{EDLC}}{C_{EDLC,\ matel}} \quad (5)$$

Where C_{EDLC} is the electric double-layer capacitance of catalysts and is determined by CVs at various scan rates.

Nitrogen isotope experiment

An isotopic labeling experiment used $^{15}N_2$ (98 atom % ^{15}N) as the feed gas to clarify the source of ammonia. After $^{15}N_2$ electroreduction for 2 h at -1.0 V (vs. RHE) and absorbed in a 0.01 M HCl solution, the obtained $^{15}NH_4^+$ was quantitatively determined by ^1H nuclear magnetic resonance (NMR, 600 MHz) with external standards, which takes methanol (CH_4O, 200 μM) as a reference.

Characterization of the Electrode

X-ray diffraction

The X-ray diffraction (XRD) spectra were obtained using a D8 powder diffractometer, which was used to characterize the change in the crystallinity. The diffractometer used Cu Kα radiation, a 30 kV tube voltage, a tube current of 20 mA, a scanning speed of 5°/min, and a scanning range of 2θ= 20° ~ 90°. Figures S5-S6 show the XRD pattern of the electrode materials loaded with nano-Fe.

Scanning electron microscopy

Scanning electron microscopy (SEM, Japan Electron Optics Laboratory) was used to analyze the surface morphology of raw and coated electrode materials. Before SEM test, samples were vacuum dried, sample detection platform and vacuum spraying gold treatment were made. Figures S7-S9 show the SEM images of the electrode materials loaded with nano-Fe.

High resolution transmission electron microscopy

In this paper, high resolution transmission electron microscopy (HRTEM, JEOL) was used to characterize the species morphology and lattice of the the three prepared electrode materials. A typical characterization process is as follows. An appropriate amount of the sample was placed into a PE tube containing anhydrous ethanol. The sample was dispersed by an ultrasonic oscillator for 5 min. The dispersion was added to a copper grid and placed under an infrared lamp to volatilize the excess ethanol. The copper grid was inserted into a transmission electron microscope, and the sample was observed and imaged using a voltage of 200 kV**.** Figures S10-S11 show the HRTEM images of three electrode materials loaded with nano-Fe.

X-ray photoelectron spectroscopy

The electron structures of metal elements in the prepared electrode materials were further examined by X-ray photoelectron spectroscopy (XPS, ESCALAB 250). Samples are pressed into sheets before testing. XPS can not only analyze the composition of elements, but also the valence of elements.

Electrochemical properties of iron based catalyst

Cyclic voltammetry curves

In the work of Zhou et al. [4], the electrode material was prepared by cyclic voltammetry, and positive results were obtained. Modified cyclic voltammetry was used to test the electrochemical activity of the electrode material in this paper. Figures S16-S19 show the cyclic voltammetry curves for electrodepositing Fe on three carrier materials and the electrochemical reduction of nitrogen to ammonia using three newly prepared catalytic materials as electrodes. Where, Figure S12 shows the cyclic voltammetry curves of the foam copper loaded with iron based catalyst.

Linear sweep voltammetry curve

In order to test the electrochemical activity of synthetic ammonia in N_2 reduction reaction, linear sweep voltammetry (LSV) tests were conducted in N_2 and Ar saturated electrolyte, as shown in Fig. 8. LSV test adopts a three electrode system, with Pt sheet as anode, SCE as reference electrode, foam copper as cathode, 0.3 M $FeSO_4$ solution as electrolyte, potential range -0.8 to -1.3 V vs. SCE, and scanning rate of 0.01 $V \cdot s^{-1}$. Figure S13 shows the linear sweep voltammetry curves of the foam copper loaded with iron based catalyst.

Chronopotentiometry

In this work, chronopotentiometry(CP) was used to evaluate the over-potential and stability of the prepared iron-based catalyst. When the current density is 10 $mA \cdot cm^{-2}$, the overpotential (η_{10}) It is one of the indicators commonly used to evaluate catalyst activity. That is to say, the higher the current density of 10 $mA \cdot cm^{-2}$ at the lower overpotential, the higher the catalyst activity.At the same time, if the current of the prepared electrode material can remain unchanged for a long time, it also indicates that the prepared electrode material is relatively stable. Figure S14 shows the Time-dependent potential curves of Fe/FC electrode at 10 mA · cm-2 in 0.3 M FeSO4 electrolyte.

Chronoamperometry

Chronoamperometry (CA) electrocatalytic synthesis of ammonia were carried out in a standard three-electrode cell electrochemical system. The reference electrode was a saturated calomel electrode (SCE), the auxiliary electrode was a platinum electrode (PE, 1 × 1 cm^2), and the working electrode (WE) was a foam copper, foam nickel and copper foil. Figures S20 show the photographs of electrochemical ammonia cell. Figure S21 show the Time-dependent current density curves of Fe/FC for ENRR at different potentials.Figure S15-S16 show the Time-dependent current density curves Fe/FC electrode with different potentials and different concentrations of $FeSO_4$ electrolyte. Figure S17 shows the photo of three-electrode electrochemical experiment. Figure S18 shows the working electrode surface pictures under different potentials. Figure S19 shows the pictures of different working electrode materials.

Electrochemical impedance spectroscopy

Electrochemical impedance spectroscopy (EIS) is to study the relationship between impedance and frequency by giving a small amplitude sinusoidal excitation in the open circuit state. In this study, Nyquist diagram is used to display EIS information. In the high frequency region, it can be used to observe the mass transfer impedance of

electrode and electrolyte, i.e. charge transfer. In the low frequency region, it can be used to observe the diffusion of ions in solution, i.e. material transfer. Figure S20 shows the Nyquist plots of Fe/FC electrode.

Results and Discussion

Supplementary Figures

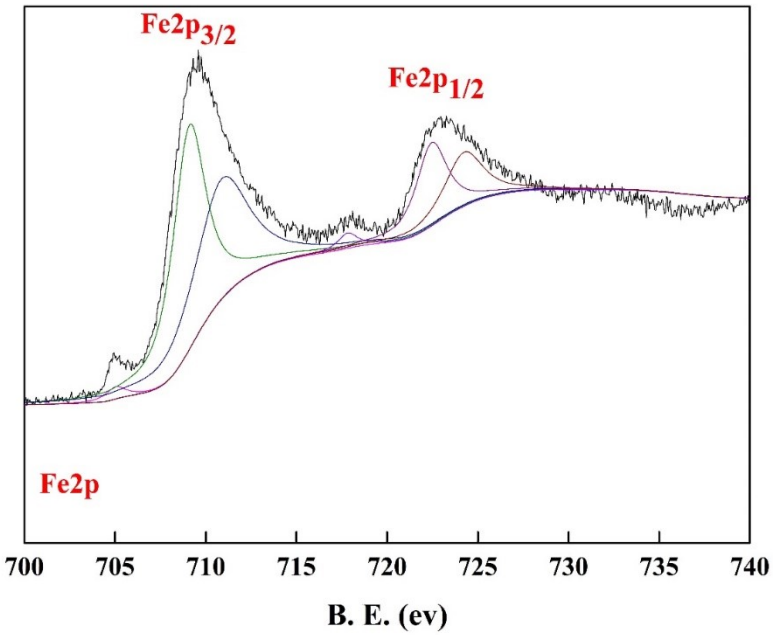

Figure S1. XPS of iron based catalyst

Figure S2. Diagram of electrochemical reaction device

Figure S3. Distillation device diagram

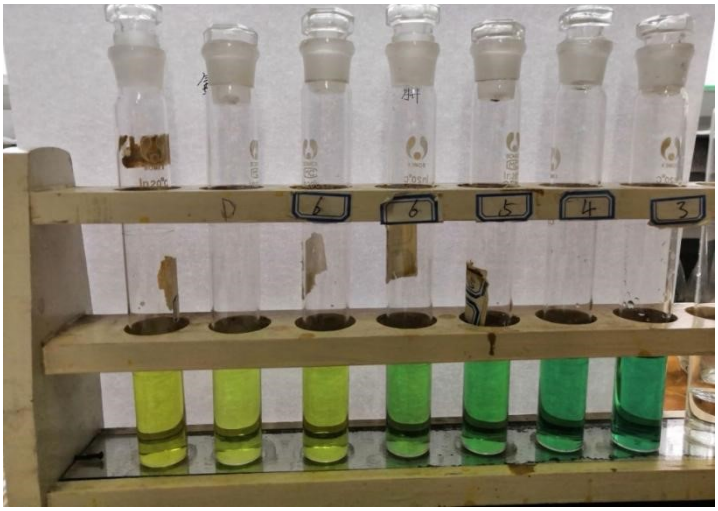

Figure S4. Photographs of standard curve for ammonia detection.

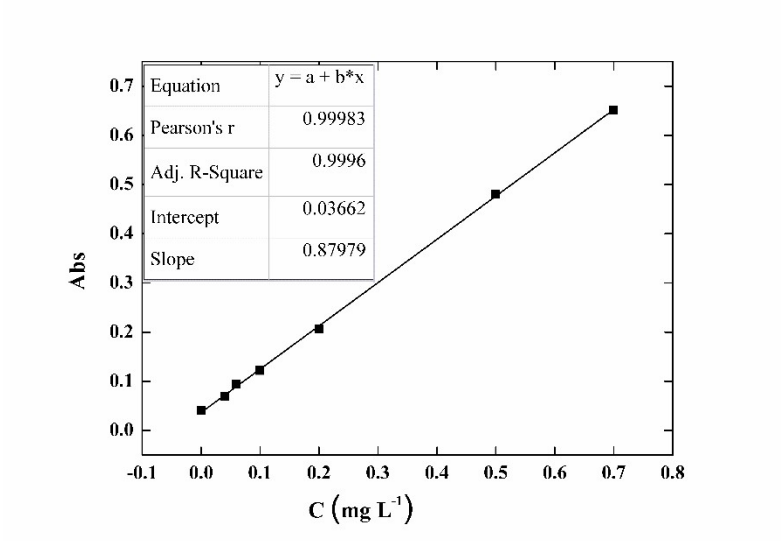

Figure S5. Standard curve for ammonia detection.

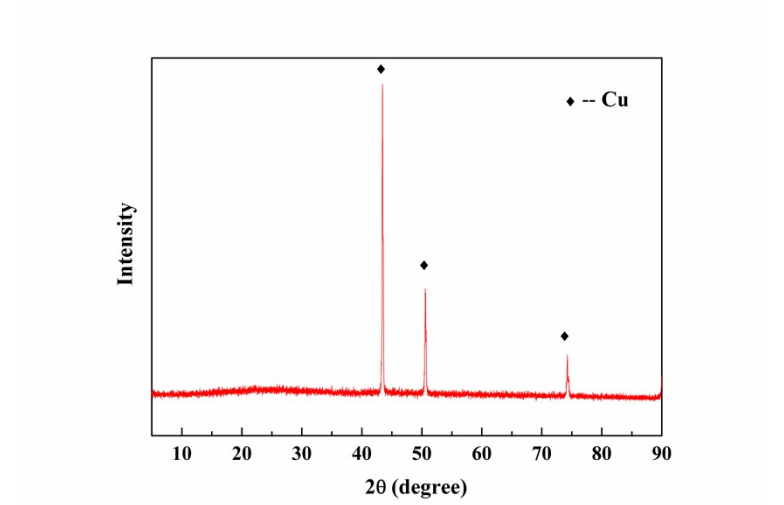

Figure S6. XRD pattern of Foam copper.

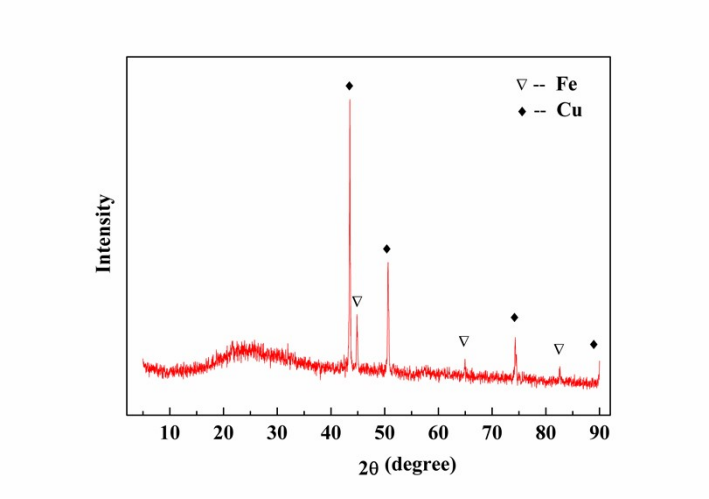

Figure S7. XRD pattern of Foam copper loaded with nano-Fe.

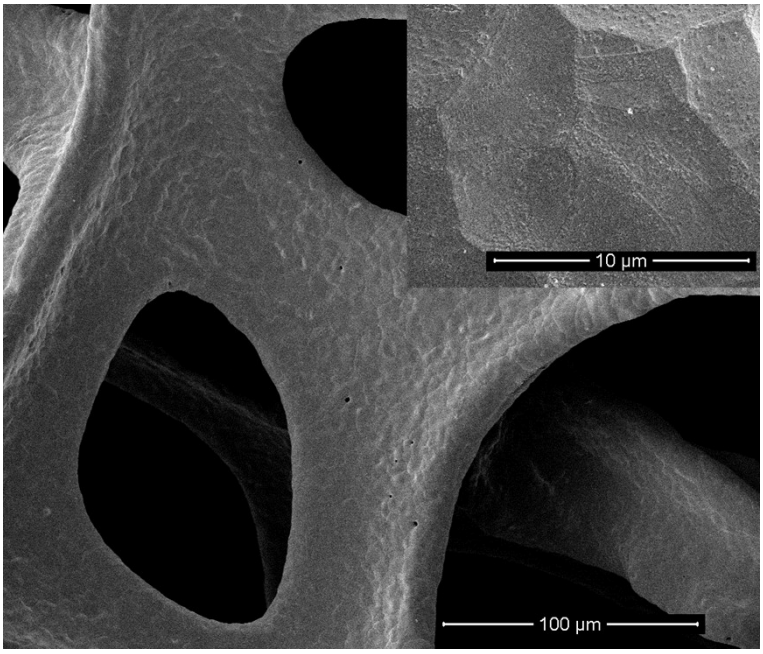

Figure S8. SEM of Pure Foam Copper Substrate.

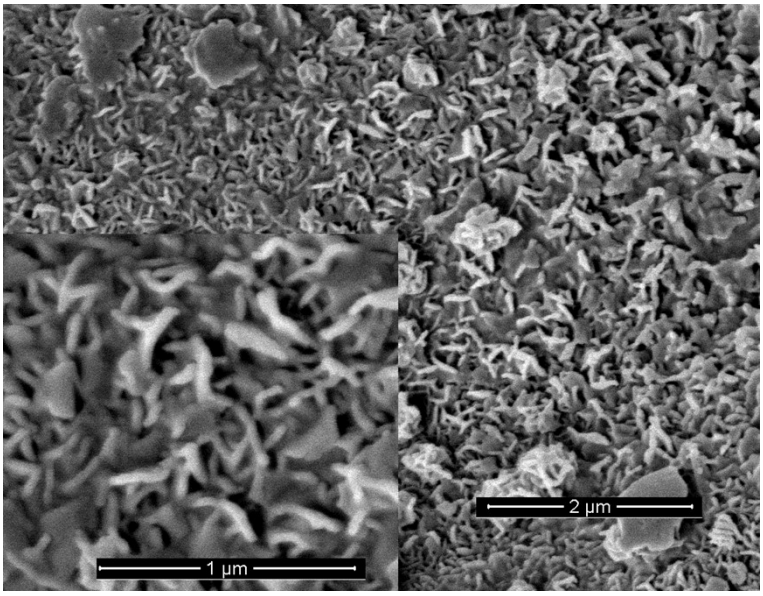

Figure S9. SEM of iron based catalyst.

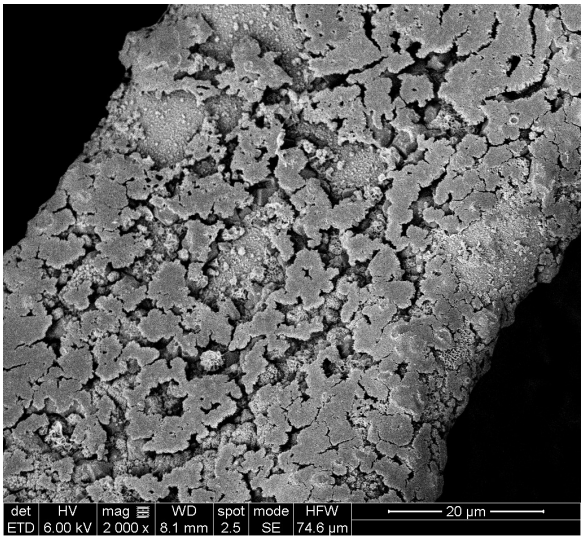

Figure S10. SEM image of Foam Copper loaded nano-Fe.

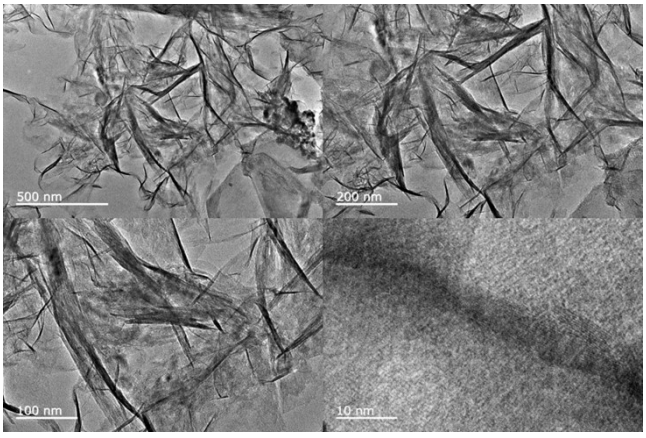

Figure S11. TEM images of Iron based Catalyst.

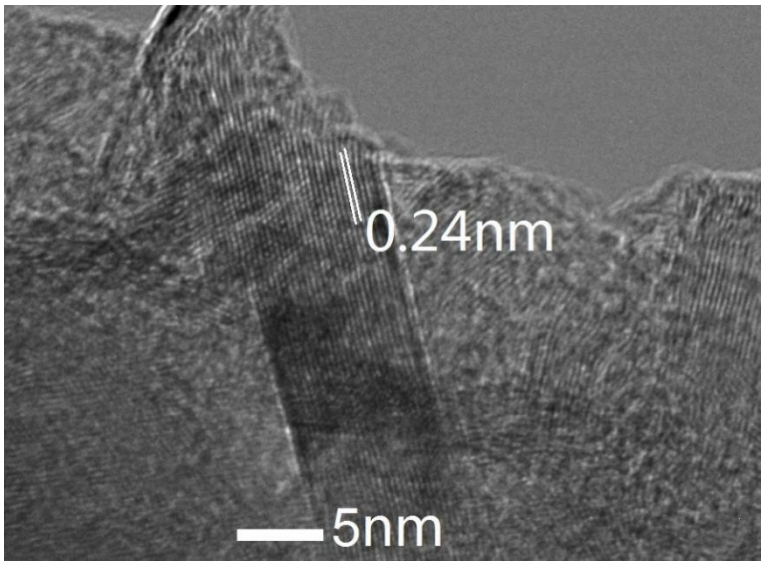

Figure S12. HRTEM image of Iron based Catalyst.

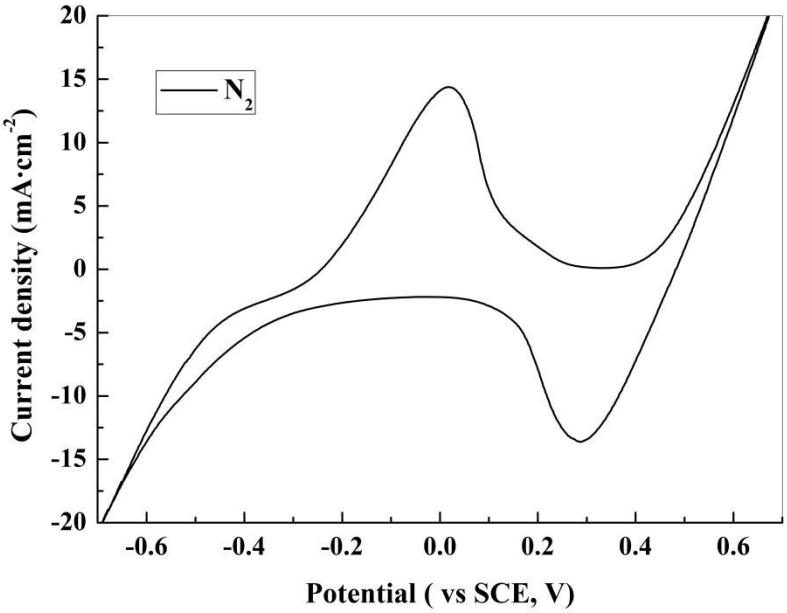

Figure S13. Cyclic voltammetry curves of Fe electrodeposited on Foam copper (80 mL of electrolyte in the electrolytic cell, the range of cyclic potential is -0.8 V-0.8 V, the voltage scanning rate is 0.02 $V \cdot s^{-1}$, and the scanning time is 5 cycles).

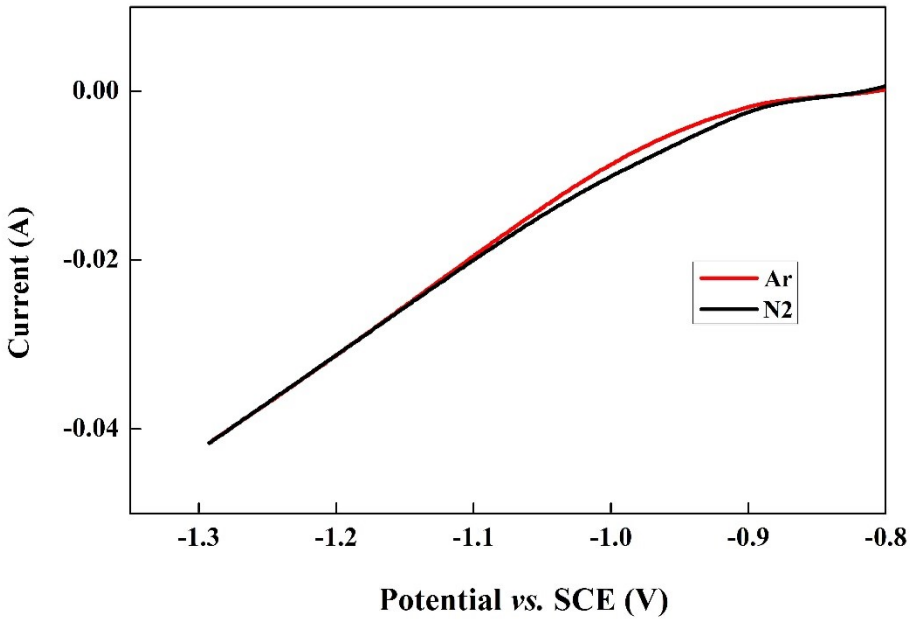

Figure S14. Linear sweep voltammetry curves of the foam copper loaded with iron based catalyst. (80 mL of electrolyte in the electrolytic cell, electrodeposition of nano-Fe by chronoamperometry with a three-electrode system; the range of cyclic potential is -1.4 V-0.8 V, the voltage scanning rate is 0.02 V·s^{-1}, and the scanning time is 5 cycles).

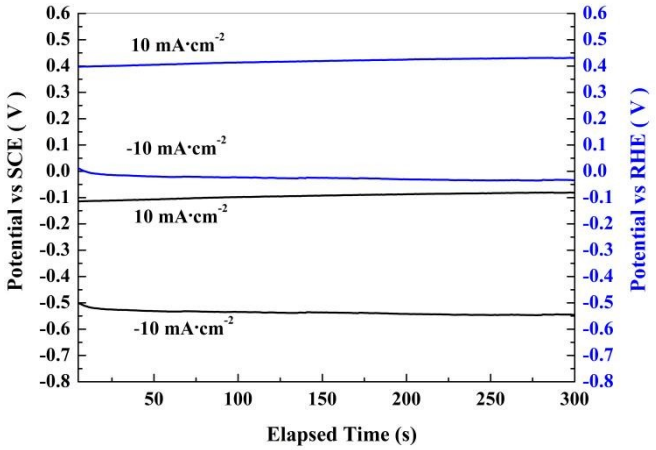

Figure S15. Time-dependent potential curves of Fe/FC electrode at 10 mA·cm^{-2} in 0.3 M $FeSO_4$ electrolyte.

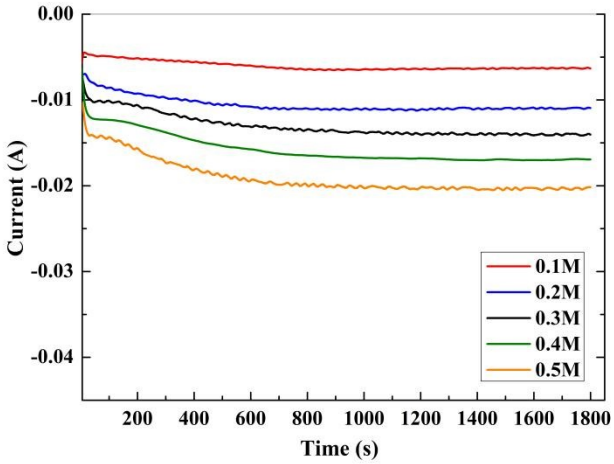

Figure S16. Time-dependent current density curves Fe/FC electrode under -1.0V vs SCE with different concentrations of $FeSO_4$ electrolyte.

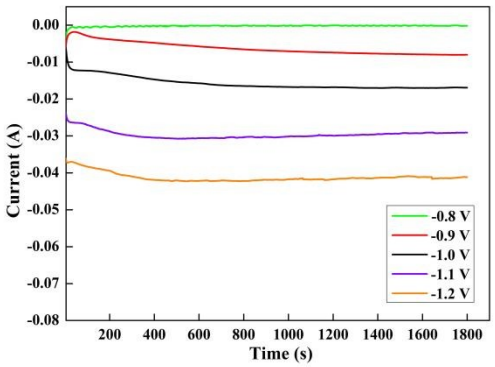

Figure S17. Time-dependent current density curves Fe/FC electrode in 0.3 M $FeSO_4$ electrolyte under different potentials.

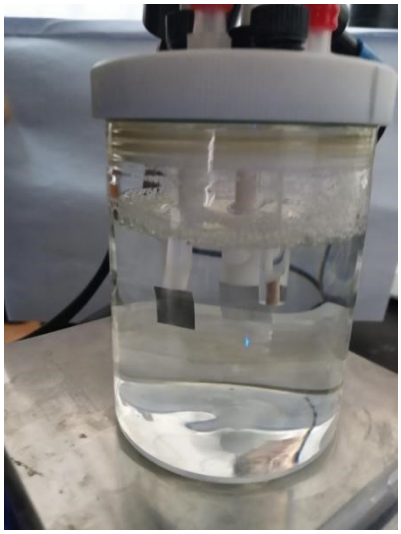

Figure S18. Photographs of electrochemical ammonia cell.

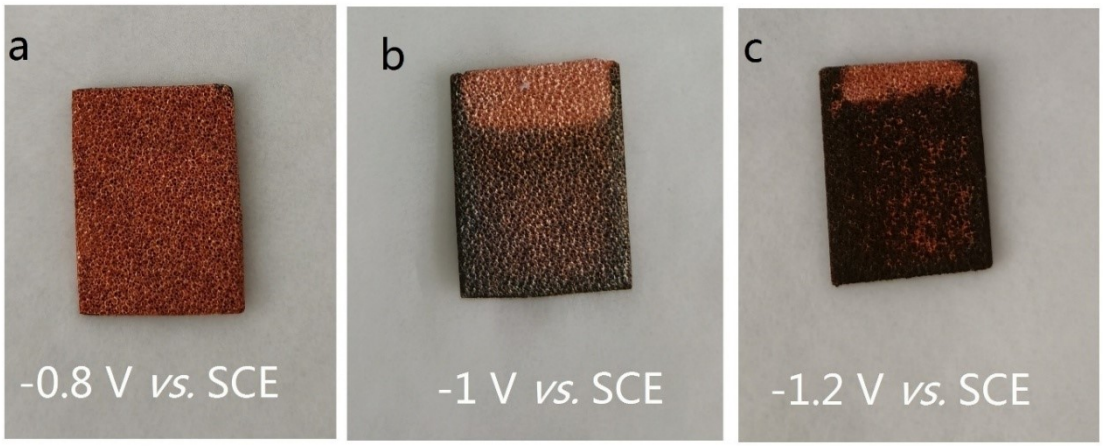

Figure S19. Working electrode surface pictures under different potentials

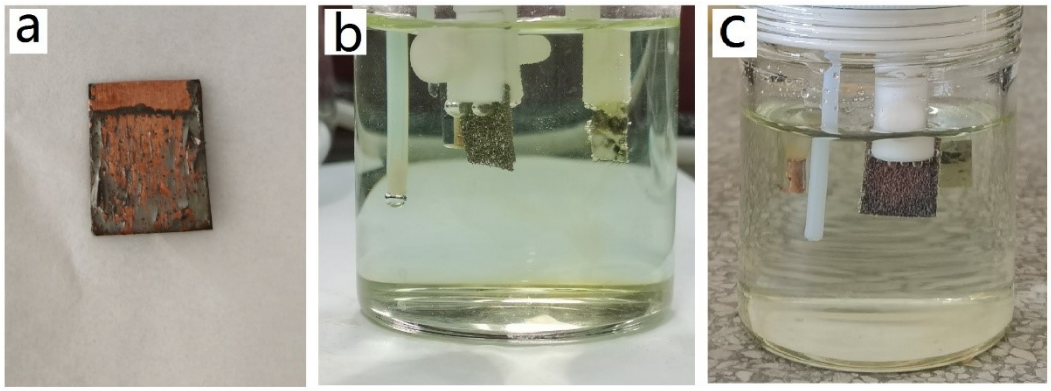

Figure S20. Different working electrode substrates (a. copper foil; b. foam nickel; c. foam copper)

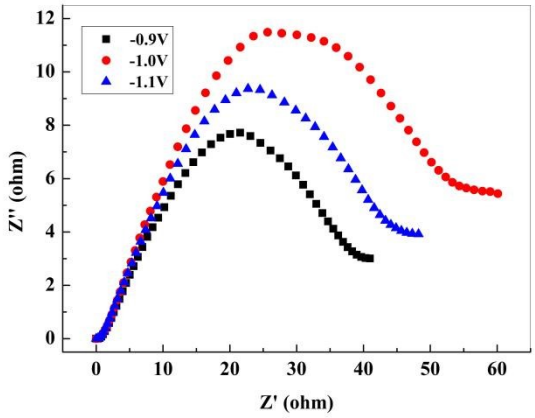

Figure S21. Nyquist plots of Fe/FC electrode

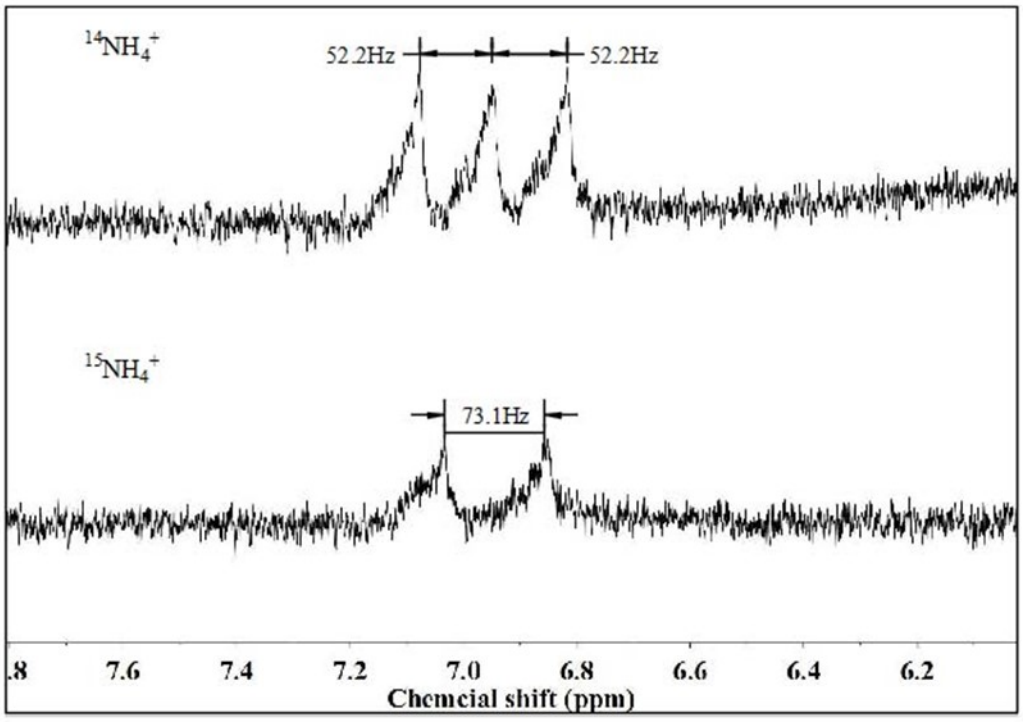

Figure S22. ^{1}HNMR spectra (600 MHz) of mixed solutions. Solutions contain equal concentrations of $^{14}NH_4^+$ and $^{15}NH_4^+$ from NH_4Cl.

Supplementary Tables

Table S1. List of solution schemes for standard curve of Indigo-phenol Blue spectrophotometry.

Tube No.	0	1	2	3	4	5	6
Ammonia standard solution（mL）	0	0.40	0.60	1.00	2.00	5.00	7.00
Absorption solution（mL）	10.00	9.60	9.40	9.00	8.00	5.00	3.00
Ammonia content（μg）	0	0.40	0.60	1.00	2.00	5.00	7.00
Ammonia concentration（$mg·L^{-1}$）	0	0.04	0.06	0.10	0.20	0.50	0.70

Table S2. The performance comparison of ENRR catalytic by different catalysts

Catalyst/working electrode	Electrolyte	T(˚C)	P(atm)	Yield rate	FE (%)	References
Fe	0.3 M $FeSO_4$ solution	25	1	923±46 $mg·h^{-1}·m^{-2}$	18.35%	This work
Fe	6N KOH	45	1	0.0002 μmol h^{-1} cm^{-2}	-	A. Sclafani, et al. **1983**[5].
Ru	Nafion	90	1	0.076	0.24	V. Kordali, et al.

				μmol h^{-1} cm^{-2}		**2000**[6].
Pt	NH_4^+ exchanged Nafion	80	1	4.10 μmol h^{-1} cm^{-2}	0.51	R. Lan, et al. **2013**[7].
Au NPS	Nafion, 0.1M KOH	25	1	0.0968 μmol h^{-1} cm^{-2}	4.0	D. Bao, et al. **2017**[8].
Au/CeOx-RGO	Nafion, 0.1M HCl	25	1	-	10.10	S. Li, et al. **2017**[9].
Au@TiO_2	Nafion, 0.1M HCl	25	1	-	8.11	M. Shi, et al. **2017**[10].
Fe_2O_3@CNT	Nafion	20	1	0.013	0.027	S. Chen, et al. **2017**[11].
Li^+-co-PEBCD	H_2SO_4 added 0.5 M Li_2SO_4, Nafion	25	1	0.11869	1.71	G. Chen, et al. **2017**[12].
γ-Fe_2O_3 NPS	0.1 M KOH	25	1	0.044	1.96	J. Kong, et al. **2017**[13].
Au	0.1 M KOH	25	1	0.014	0.12	Y. Yao, et al. **2018**[14].
CNS(N-doped carbon nonaspikes)	0.25 M $LiClO_4$	25	1	5.71±0.42	11.56±0.85	Y. Song, et al. **2018**[15].
Mxene/FeOOH nanosheets	0.5 M Li_2SO_4 solution	25	1	0.26 μg h^{-1} cm^{-2}	5.78	Y. Luo, et al. **2019**[16].
MXene/SSM	0.5 M Li_2SO_4 solution	25	1	4.72 μg h^{-1} cm^{-2}	4.62	L. Huang, et al. **2019**[17].
Nano-Fe	K_3PO_4 solution	25	1	0.79 nmol s^{-1} cm^{-2}	16.68	Q. Zhang, et al. **2020**[18].
Fe_2O_3 (Ni-monel electrode)	Molten NaOH/KOH	200	1	8.64 μg h^{-1} cm^{-2}	35	S. Licht, et al. **2014**[19]
Fe_2O_3/AC (stainless steel electrode)	Molten NaOH/KOH	250	1	29.8 μg h^{-1} cm^{-2}	4.9	B. Cui, et al. **2017**[20].
Mo_2C/C	0.5 M Li_2SO_4 solution	25	1	11.3 μg h^{-1} mg^{-1}_{Mo2C}	7.8	H. Cheng, et al. **2018**[21].
FL-BP NSs	0.01 M HCl solution	25	1	31.37 mg $h^{-1}mg^{-1}cat$	5.07	L. Zhang, et al. **2019**[22].
Bi nanocrystals	0.5 M K_2SO_4	25	1	0.052 mmol cm^{-2} h^{-1}	66	Y. Hao, et al. **2019**[23].
$CoMoO_4$	0.10 M Na_2SO_4	25	1	79.87 mmol h^{-1} $gcat.^{-1}$	22.76	Y. Zhang, et al. **2021**[24].
Fe SAs/MoS_2	0.1 M KCl	25	1	36.1 mmol h^{-1} $mgcat^{-1}$	31.6	J. Li, et al. **2020**[25].
Fe-FTO	ionic liquids	25	1	2.9 mg m^{-2} h^{-1}	60	F. Zhou, et al. **2017**[26].
Fe-C/ Fe-SSM	ionic liquids	25	1	103.6 mg m^{-2} h^{-1} /56.0 mg m^{-2} h^{-1}	20/60	Q. Zhang, et al. **2021**[27].
Copper disk	0.2 M $LiBF_4$ + 0.1 M IL	24±2	19.5-bar	53±1nmols-1cm-2	69±1	Bryan H. R.

	solutions in THF					Suryanto, et al. **2021**[28].
Ag-Au@ZIF	0.2 M $LiCF_3SO_3$ in THF	25	1	6 $pmolcm^{-2}s^{-1}$	90	H. K. Lee, et al. **2018**[29].
Stainless steel cloth	1 M LiClO4 in THF-DEE	25	1	37.48±3.52 nmol cm^{-2} s^{-1}.	54.78±1.60	Y. Li, et al. **2024**[30].

References

[1] M. W. Weatherburn, *nal. Chem.* **1967**, 39(8): 971-974.
[2] L. Zhou, C. E. Boyd, *Aquaculture* **2016**, 450, 187-193.
[3] G. W. Watt, J. D. Chrisp, *Anal. Chem.* **1952**, 24(12), 2006-2008.
[4] F. Zhou, et al., *Energ. Environ. Sci.* **2017**, 10, 2516-2520.
[5] A. Sclafani, et al., J. Electrochem. Soc. **1983**, 130, 734-736.
[6] V. Kordali, et al., Chem. Commun. **2000**, 1673-1674.
[7] R. Lan, et al., Sci. Rep. **2013**, 3, 1145.
[8] D. Bao, et al., Adv. Mater. **2017**, 29, 1604799.
[9] S. Li, et al., Adv. Mater. **2017**, 29, 1700001.
[10] M. Shi, et al., Adv. Mater. **2017**, 29, 1606550.
[11] S. Chen, et al., Angew. Chem. Int. Ed. **2017**, 56, 2699-2703.
[12] G. Chen, et al., J. Am. Chem. Soc. **2017**,139, 9771-9774.
[13] J. Kong, et al., ACS Sustainable Chem. Eng. **2017**, 5, 10986-10995.
[14] Y. Yao, et al., J. Am. Chem. Soc. **2018**, 140, 1496-1501.
[15] Y. Song, et al., Sci. Adv. **2018**, 4, e1700336.
[16] Y. Luo, et al., Joule **2019**, 3. 279-289.
[17] L. Huang, et al., Chem **2019**, 5, 15-17.
[18] Q. Zhang, et al., ChemCatChem **2020**, 12, 334-341.
[19] S. Licht, et al., Science **2014**, 345, 637-640.
[20] B. Cui, et al., Green Chem. **2017**, 19,298-304.
[21] H. Cheng, et al., Adv. Mater. **2018**, 30, 1803694.
[22] L. Zhang, et al., Angew. Chem. Int. Ed. **2019**, 58, 2612-2616.
[23] YC. Hao, et al., Nat Catal **2019**, 2, 448-456.
[24] Y. Zhang, et al., J. Mater. Chem. A **2021**, 9, 5060-5066.
[25] J. Li, et al., Chem **2020**, 6, 1-17.
[26] F. Zhou, et al., Energy Environ. Sci. **2017**, 10, 2516-2520.
[27] Q. Zhang, et al., Green Chem. **2021**, 23, 7685-7691.
[28] Bryan H. R. Suryanto, et al., Science **2021**, 372, 1187-1191.
[29] H. K. Lee, et al., Sci. Adv. **2018**, 4, eaar32.
[30] Y. Li, et al., Angew. Chem. Int. Ed. **2024**, 63, e202311413.

Author Contributions

Q. Zhang conceived and supervised the project. Q. Zhang and K. Chen designed the project. K. Chen, R. Deng and C. Zhao conducted electrochemical synthesis of ammonia reactions and XRD, XPS, SEM, HRTEM and Ammonia measurements. Q. Zhang, K. Chen and C. Zhao analyzed the data, interpreted the results, and wrote the manuscript. All authors proofread the manuscript.